

Optical conductivity and resistivity of a hole-doped spin-fermion model for cuprates

Mohammad Moraghebi,¹ Seiji Yunoki,² and Adriana Moreo¹

¹*Department of Physics, National High Magnetic Field Lab and MARTECH, Florida State University, Tallahassee, Florida 32306*

²*Istituto Nazionale di Fisica della Materia and International School for Advanced Studies (SISSA), via Beirut 4, Trieste, Italy*

(Received 9 May 2002; published 30 December 2002)

The optical conductivity and Drude weight of a spin-fermion model for cuprates are studied as a function of electronic density and temperature using Monte Carlo techniques. This model develops stripes and robust *D*-wave pairing correlations upon hole doping, and it has the advantage that it can be numerically simulated without sign problems. Both static and dynamical information can be obtained. In this work, it was possible to analyze up to 12×12 site clusters at low temperatures ranging between $0.01t$ and $0.1t$ (between 50 K and 500 K for a hopping amplitude $t \sim 0.5$ eV). As the temperature is reduced, spectral weight is transferred from high to low frequencies in agreement with the behavior observed experimentally. Varying the hole density, the Drude weight has a maximum at the optimal doping for the model, i.e., at the density where the pairing correlations are stronger. It was also observed that the inverse of the Drude weight, roughly proportional to the resistivity, decreases *linearly* with the temperature at optimal doping, and it is abruptly reduced when robust pairing correlations develop upon further reducing the temperature. The behavior and general form of the optical conductivity are found to be in good agreement with experimental results for the cuprates. Our results also establish the spin-fermion model for cuprates as a reasonable alternative to the *t*-*J* model, which is much more difficult to study accurately.

DOI: 10.1103/PhysRevB.66.214522

PACS number(s): 74.25.Gz, 71.10.Fd

I. INTRODUCTION

Infrared measurements are an important probe of the dynamical properties of the high critical temperature superconducting cuprates. In particular, the real part of the optical conductivity $\sigma(\omega)$ provides useful insight into the electronic structure of these materials.¹⁻³ Measurements of the optical conductivity have been performed in both hole- and electron-doped cuprates. Common features observed include the absence of absorption below the charge-transfer gap in the insulating phase (half-filling). The rapid transfer of spectral weight to low frequencies with increasing hole doping has also been reported, which gives rise to a Drude-like peak at $\omega=0$ and a broad mid-infrared feature, while the spectral weight above the charge-transfer gap decreases.^{2,3} The reported integrated conductivity up to 4 eV (beyond the charge-transfer gap) in $\text{La}_{2-x}\text{Sr}_x\text{CuO}_4$ remains approximately constant with doping, indicating that spectral weight is redistributed from the charge-transfer band to lower frequencies.³ It is also observed that at low frequencies, $\sigma(\omega) \approx 1/\omega$ instead of the $1/\omega^2$ behavior expected in a standard metal.

A number of the above-mentioned features are well reproduced by models of strongly correlated electrons, including the Hubbard, *t*-*J*, and related Hamiltonians,^{4,5} even in regimes where superconductivity was not numerically detected in the ground state. This suggests that some of the previously described properties of cuprates may just be the effect of strong correlations among the electrons, rather than superconductivity that is expected to develop at much lower temperatures than those previously studied. A problem in the calculation of the optical conductivity in Hubbard and *t*-*J* models is that only small clusters of about 20 sites can be studied with exact diagonalization techniques.^{6,7} Alternative approaches, such as the quantum Monte Carlo method allows

the analysis of larger clusters (8×8), but at very high temperatures and with less precision.⁸ However, recent investigations have shown that these problems can be overcome by using a spin-fermion model (SFM), which is much easier to study numerically. In fact, those previous investigations have reported on the presence of a stable striped ground state upon doping, and robust *D*-wave pairing correlations in the SFM.⁹⁻¹² It has been observed that vertical and horizontal stripes with an electronic density of about 50% develop due to the competition between the antiferromagnetic (AF) phase, which naturally appears at half-filling, and the tendency of the holes to form clusters in order to minimize the disruption that they cause to the AF background. The stripes have been observed in snapshots during the numerical simulations, and they manifest also in the behavior of the charge structure factor.¹² Recent computational evaluations of the *D*-wave pairing correlations given by $C_D(\mathbf{r}) = \langle \hat{\Delta}_{\mathbf{i}+\mathbf{r}}^D \hat{\Delta}_{\mathbf{i}}^{D\dagger} \rangle$ have revealed robust long-distance pairing upon doping in the direction perpendicular to the stripes.¹¹ Here the pairing operator is given by $\hat{\Delta}_{\mathbf{i}}^D = \sum_{\alpha} \sum_{\hat{e}=\pm\hat{x},\pm\hat{y}} \alpha e c_{\mathbf{i},\alpha} c_{\mathbf{i}+\hat{e},-\alpha}$, where $e=1$ for $\hat{e}=\pm\hat{x}$, $e=-1$ for $\hat{e}=\pm\hat{y}$, and α is the spin projection.

The presence of phenomenologically observed regimes of the high- T_c cuprates in a simple model of interacting mobile carriers and localized spins is remarkable, and opens the way to detailed numerical investigations of relevant physical quantities. In this context, clusters as large as 12×12 can be investigated for low temperatures ranging between $0.01t$ and $0.1t$, considerably improving upon size and temperature limitations of the *t*-*J* and Hubbard models. In particular, the effect of the stripes on $\sigma(\omega)$ and its distribution of spectral weight, and dependence with temperature can be studied in this case, as reported here.

The organization of the paper is as follows. In Sec. II the

Hamiltonian and the numerical technique are described. Results at $T \approx 0$ are discussed in Sec. III, while Sec. IV is devoted to the finite temperature analysis. An estimation of the linear dc resistivity is presented in Sec. V, and the conclusions appear in Sec. VI.

II. MODEL AND TECHNIQUE

The SFM is constructed as an interacting system of electrons and spins, which mimics phenomenologically the coexistence of charge and spin degrees of freedom in the cuprates.^{13,14,5} Its Hamiltonian is given by

$$H = -t \sum_{\langle ij \rangle \gamma} (c_{i\gamma}^\dagger c_{j\gamma} + \text{H.c.}) + J \sum_{\mathbf{i}} \mathbf{s}_{\mathbf{i}} \cdot \mathbf{S}_{\mathbf{i}} + J' \sum_{\langle ij \rangle} \mathbf{S}_{\mathbf{i}} \cdot \mathbf{S}_{\mathbf{j}}, \quad (1)$$

where $c_{i\gamma}^\dagger$ creates an electron at site $\mathbf{i} = (i_x, i_y)$ with spin projection γ , $\mathbf{s}_{\mathbf{i}} = \sum_{\gamma\beta} c_{i\gamma}^\dagger \boldsymbol{\sigma}_{\gamma\beta} c_{i\beta}$ is the spin of the mobile electron, the Pauli matrices are denoted by $\boldsymbol{\sigma}$, $\mathbf{S}_{\mathbf{i}}$ is the localized spin at site \mathbf{i} , $\langle ij \rangle$ denotes nearest-neighbor (NN) lattice sites, t is the NN-hopping amplitude for the electrons, $J > 0$ is an AF coupling between the spins of the mobile and localized degrees of freedom, and $J' > 0$ is a direct AF coupling between the localized spins. The density $\langle n \rangle = 1 - x$ of itinerant electrons is controlled by a chemical potential μ . Hereafter, $t = 1$ will be used as the unit of energy. From previous phenomenological analysis, and as in previous papers,^{9,12} the coupling $J = 2$ and the Heisenberg coupling $J' = 0.05$ are selected, since they provide the striped and pairing states observed in cuprates. To simplify the numerical calculations, avoiding the sign problem, localized spins are assumed to be classical (with $|\mathbf{S}_{\mathbf{i}}| = 1$). This approximation is not as drastic as it appears, and it has been extensively discussed in detail in previous publications such as Ref. 12. The model will be studied using a Monte Carlo method, details of which can be found in Ref. 15. Periodic boundary conditions (PBC) are used.

The real part of the optical conductivity is calculated¹⁶ as

$$\sigma_{\alpha\alpha}(\omega) = \frac{(1 - e^{-\beta\omega})}{\omega} \frac{\pi}{Z} \sum_{n,m} e^{-\beta E_n} |\langle n | J_\alpha | m \rangle|^2 \times \delta(\omega + E_n - E_m), \quad (2)$$

where $\alpha = x, y$; Z is the partition function; $|n\rangle$ and $|m\rangle$ denote eigenstates of the system; and J_α is the current operator given by

$$J_\alpha = \frac{it}{2} \sum_{\mathbf{r}\sigma} (c_{\mathbf{r}+\alpha,\sigma}^\dagger c_{\mathbf{r},\sigma} - c_{\mathbf{r},\sigma}^\dagger c_{\mathbf{r}+\alpha,\sigma}). \quad (3)$$

Since we are using PBC, the Drude weight D_α is calculated indirectly, using the two-dimensional sum rule,

$$\int_0^\infty d\omega \sigma_{\alpha\alpha}(\omega) = \frac{\pi}{2N} \langle -K_\alpha \rangle, \quad (4)$$

where $\langle -K_\alpha \rangle$ is the average kinetic energy in the direction α and N is the number of sites in the lattice. Assuming the existence of a contribution $D\delta(\omega)$ at zero energy, we obtain

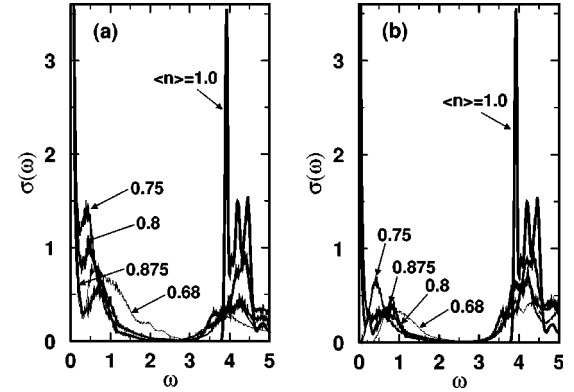


FIG. 1. (a) The optical conductivity versus ω at $T = 0.01$ in the direction perpendicular to the stripes and different densities on a 12×12 cluster. (b) Same as (a), but in the direction parallel to the stripes.

$$\frac{D_\alpha}{\pi} = \frac{\langle -K_\alpha \rangle}{2N} - \frac{1}{\pi} \int_0^\infty d\omega \sigma_{\alpha\alpha}(\omega). \quad (5)$$

This procedure to calculate the Drude weight is a common practice, and it has been discussed extensively in reviews.⁷ In this work, both directions x and y must be analyzed independently since at low temperature, $T < 0.025t$, the symmetry under rotations is broken due to the formation of stripes. As a consequence, the optical conductivity will be measured along the direction parallel and perpendicular to those stripes.

In numerical calculations of the optical conductivity, it is customary to replace the δ functions in Eq. (2) by Lorentzians of width ϵ . The smearing of the δ 's helps to simulate effects not considered in the microscopic Hamiltonians, such as disorder that contributes to the experimentally observed broadening of the peaks.⁷ This peak broadening also occurs naturally in the Monte Carlo simulations since the position of the poles varies slightly between successive iterations. Here, the incoherent part of the optical conductivity is calculated by effectively giving a width $\epsilon \approx 0.01t$ to the delta functions. That same value of ϵ will be used in the Lorentzian for the Drude weight.

III. RESULTS AT $T \sim 0$

In Fig. 1(a), we present the real part of the optical conductivity measured in the direction perpendicular to the stripes on a 12×12 lattice¹⁷ at $T = 0.01t$ for different values of the electronic density $\langle n \rangle$. At half-filling, all the spectral weight appears beyond $\omega \approx 3.8t$. This corresponds to about 2 eV if we assume $t \approx 0.5$ eV, in agreement with experimental results. This half-filling gap is created by the coupling J , which plays a role analogous to U in the Hubbard model. In fact, J suppresses double occupancy of the mobile carriers as strongly as U does. This important point has been extensively discussed particularly in the manganite literature where a similar model, but with different signs and values of couplings, is used to describe e_g electrons moving in a t_{2g} background.¹⁸

For $\langle n \rangle = 0.875$, spectral weight is observed at low values

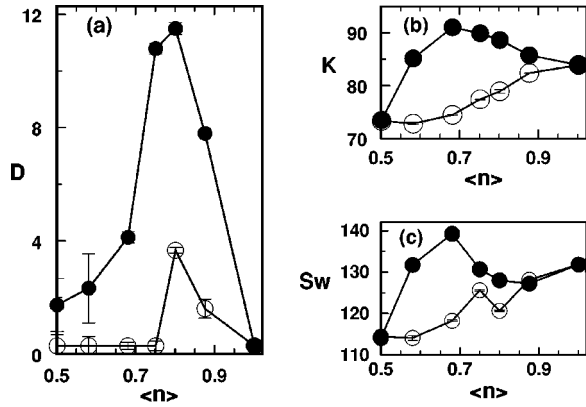


FIG. 2. (a) The Drude weight as a function of the electronic density at $T=0.01$ for currents perpendicular (parallel) to the stripes denoted by filled (open) circles. (b) The kinetic energy as a function of the electronic density at $T=0.01$ in the direction perpendicular to the stripes (filled circles) and parallel to them (open circles). (c) Integral of the incoherent spectral weight of $\sigma(\omega)$ versus the electronic density, calculated along the direction perpendicular (filled circles) and parallel (open circles) to the stripes.

of ω , again as in the experimental data for the cuprates. In the same figure, data for $\langle n \rangle = 0.80, 0.75$, and 0.68 are shown. It can be observed that spectral weight is transferred from above the gap to low energies in all cases. At the same time, the Drude weight D , shown in Fig. 2(a) with filled circles, becomes finite with doping, indicating that the system transforms from an insulator to a conductor.¹⁹ Notice that D reaches its maximum value for $\langle n \rangle \approx 0.75-0.80$. According to previous investigations, this corresponds to the optimal doping for the SFM, i.e., these are the densities at which the D -wave pairing correlations are the strongest.¹¹ The maximum obtained in the Drude weight is due to the interplay between the kinetic energy and the incoherent spectral weight, which are shown in Figs. 2(b) and 2(c), respectively. It is interesting to notice that in previous studies performed on the large- U Hubbard and t - J models, it was observed that the kinetic energy reaches a maximum at quarter filling in regimes without stripes.²⁰ However, in the SFM, the kinetic energy perpendicular to the stripes has a maximum for $\langle n \rangle \approx 0.7$ [see Fig. 2(b)]. This is in agreement with experimental results which found that the plasma frequency, proportional to the kinetic energy, grows with doping in the underdoped region and stops growing at optimal doping.²¹ This also establishes an important difference between previous t - J model studies and those reported here.

It has also been observed that in the direction parallel to the stripes, the conduction is much suppressed, as it can be seen in Fig. 1(b). This is in agreement with previous dynamical studies of the model, which showed that the kinetic energy is larger in the direction perpendicular to the stripes,¹⁰ as appears also in Fig. 2(b). It is also clear that the kinetic energy continuously decreases with doping in the parallel direction. The corresponding Drude weight is denoted with open circles in Fig. 2(a).

IV. RESULTS AT FINITE TEMPERATURE

The next step is to study the dependence of the optical conductivity with temperature. Experimental measurements

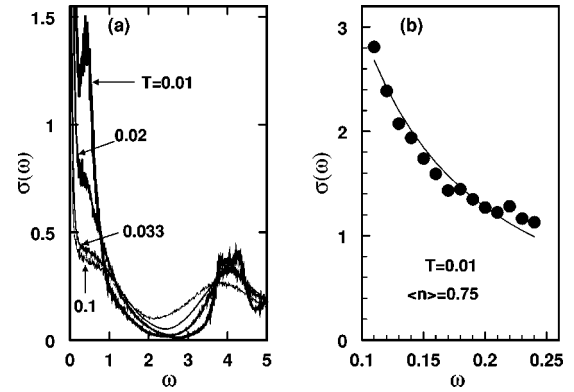


FIG. 3. (a) The optical conductivity of the spin-fermion model versus ω at $\langle n \rangle = 0.75$ in the direction perpendicular to the stripes and different temperatures on a 12×12 cluster. The temperatures are indicated; (b) Details of the curve shown in part (a) for $T = 0.01t$, where the data for $0.1 < \omega < 0.25$ are fitted by an $1/\omega$ curve.

have been carried out mainly in a narrow range between 0.01 and 0.25 eV, which corresponds to $\omega < 0.50$ in our scale. For $\text{La}_{2-x}\text{Sr}_x\text{CuO}_4$ (LSCO), measurements have been reported for $x = 0.13$ and 0.14 (underdoped) and $x = 0.22$ (overdoped) at temperatures ranging between 10 K and 400 K,²² while underdoped Bi2212 and optimally doped Y123 have also been studied.²³

In the underdoped case, it has been experimentally observed that as the temperature decreases from 400 K, spectral weight is transferred from intermediate towards lower frequencies. This depletion of spectral weight is associated with the opening of a pseudogap in the density of states at a temperature T^* estimated to be above 400 K. In the overdoped and optimally doped samples, on the other hand, the depletion of spectral weight is observed below T_c , indicating that $T^* \approx T_c$ in this case.²³

In Fig. 3(a), the optical conductivity versus ω is shown at optimal doping $\langle n \rangle = 0.75$ for different temperatures. Based on the previous studies of D -wave pairing correlations, the critical temperature is $T_c \approx 0.025$. It can be clearly seen that spectral weight is transferred to lower frequencies as the temperature decreases. The mid-infrared (MIR) weight increases, as well as the Drude weight, whose inverse is displayed in Fig. 4 as a function of temperature.

The MIR feature is characteristic of doped cuprates, and it is located at $\omega \approx 0.3$ eV.²⁴ This is in very good agreement with our results presented in Figs. 1(a) and 3(a), where the MIR feature appears for $\omega \approx 0.5-0.8$, which corresponds to $0.25-0.40$ eV for $t = 0.5$ eV.

As mentioned before, it was experimentally observed that at low frequencies (above $\omega \approx 0.03$ eV), the decrease in the conductivity is closer to $1/\omega$ than $1/\omega^2$, which would have been expected for free carriers. The best fit of our data for $\sigma(\omega)$ in the range $0.1 < \omega < 0.25$ with a power law C/ω^α corresponds to $0.9 < \alpha < 1.3$, in all the range of temperatures and dopings studied, in excellent agreement with the experimental results. In Fig. 3(b) we show, as an example, the $1/\omega$

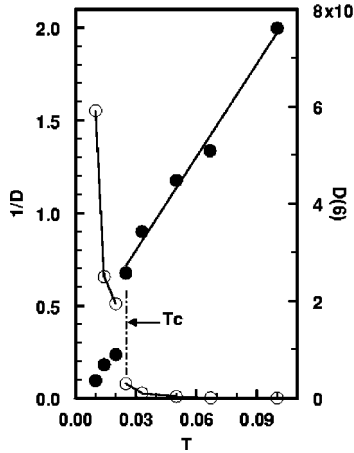


FIG. 4. The inverse of the Drude weight (filled circles, scale on the left) as a function of the temperature, for the optimal doping $\langle n \rangle = 0.75$, and for currents perpendicular to the stripes. The line indicates a linear fit. The open circles indicate the D -wave pairing correlation at the maximum distance $D(6)$ (scale on the right). The qualitative agreement with cuprate's experiments is evident.

fit for the data at optimal doping and $T = 0.01t$. It appears that the mixture of Drude weight and MIR band at low frequencies produces the $1/\omega$ behavior.

V. ESTIMATION OF THE RESISTIVITY

It has already been mentioned that the effects of dissipative processes that would create a finite resistance in a metal have to be added *ad hoc*, by replacing the δ functions at $\omega = 0$ by Lorentzians, since these processes are not included in the Hamiltonian of the spin-fermion model. Once this is done, the inverse of the Drude weight should provide information about the dc resistivity ρ_{dc} .⁶ Transport experiments indicate that a linear behavior occurs for $T > T^*$, while in the pseudogap region of the underdoped compounds, a faster decrease of ρ_{dc} is found for $T_c < T < T^*$.^{22,25} A power-law dependence $\rho_{dc} \approx T^{1+\delta}$ was observed in the overdoped regime with $\delta = 0.5$ at 34% doping in LSCO that is optimally doped at 15%.²⁵

It is remarkable that many of the above-mentioned experimental characteristics are qualitatively captured by the SFM. In particular, in Fig. 4, a *linear* fit of our data at optimal doping is obtained above T_c (filled circles). Notice that, in principle, since no dissipative processes are included in the Hamiltonian, it is not possible to determine the onset of superconductivity by studying $1/D$ as a function of the temperature, since we cannot distinguish between a perfect metal and a superconductor by monitoring the Drude weight in this case. However, we observe a rapid reduction of $1/D$ at T_c (see Fig. 4). This reduction occurs as the D -wave pairing correlations develop a robust value at long distances. The longest distances in our clusters is $L = 6$, and as a consequence $D(6)$ is also shown in Fig. 4 as a function of the temperature (open circles). In this case, $T_c = 0.025t \approx 150$ K, which is the temperature for which a pseudogap¹² opens in the density of states, completing an impressive agreement with cuprate's phenomenology.

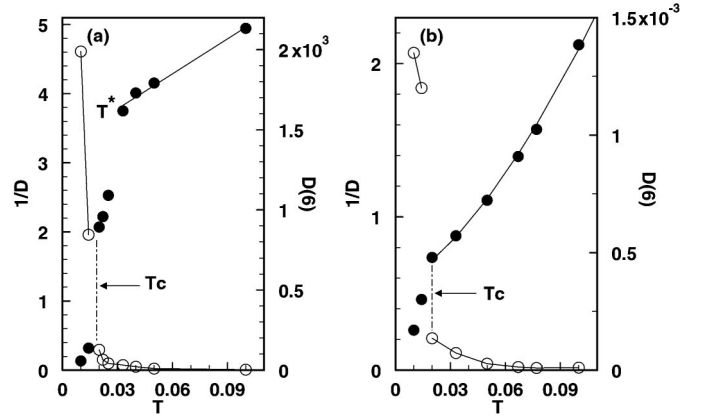


FIG. 5. (a) Same as Fig. 4 but for $\langle n \rangle = 0.875$ (underdoped). The continuous line is a linear fit of the $1/D$ points above T^* ; (b) Same as Fig. 4 but for $\langle n \rangle = 0.68$ (overdoped). The continuous line is a $T^{1.5}$ fit of the $1/D$ points above T_c .

Behavior in qualitative agreement with the experiments is also observed away from optimal doping. In our underdoped regime, with a representative density $\langle n \rangle = 0.875$, the inverse of the Drude weight and the $D(6)$ pairing correlation are shown as a function of temperature in Fig. 5(a). In this case, linear behavior reducing T is observed up to $T = 0.033t \approx 200$ K when a pseudogap starts developing in the density of states. Thus, this temperature may be associated to the experimental T^* . Below this temperature, the slope of $1/D$ increases and a further reduction of the resistivity is observed at $T_c = 0.017t \approx 100$ K, which is the temperature where the $D(6)$ pairing correlations start to develop. This is in qualitative, although not quantitative, agreement with the experimental data for $\text{La}_{2-x}\text{Sr}_x\text{CuO}_4$.

Data in the overdoped regime, for $\langle n \rangle = 0.68$, are displayed in Fig. 5(b). As in the previous two cases, a sharp decrease in $1/D$ is observed at T_c when the $D(6)$ pairing correlations start to increase. However, above T_c , we observe indications of superlinear behavior like in the experiments.²⁵

On the other hand, while the onset of superconductivity is very obvious in resistivity measurements, it is not clear that the incoherent part of the optical conductivity is sensitive to it, particularly in the overdoped regime. The transference of spectral weight from higher to lower frequencies observed as the temperature decreases has been associated to the opening of the pseudogap rather than to the onset of superconductivity. No particular feature is observed at T_c in this case.²²

An interesting characteristic of the SFM results is that spectral weight is transferred to lower frequencies when the temperature decreases, as experimentally observed in the cuprates. This behavior is not obvious. In fact, since the SFM develops stripes, i.e., charge ordering, at low temperatures one possible behavior would have been that spectral weight was transferred towards higher frequencies when the temperature decreases, which is the expected behavior for systems that develop charge-density waves.

VI. CONCLUSIONS

Summarizing, the optical conductivity of the SFM appears to have many features in common with those of the

high- T_c cuprates. A transference of spectral weight from high to low frequencies is observed upon doping. The Drude weight reaches its maximum value at optimal doping and its inverse, roughly proportional to the resistivity, decreases linearly with temperature in this regime. Qualitative agreement with the experimental behavior of the resistivity is also observed in the underdoped and overdoped cases. The simplicity of the SFM allows the study of larger clusters than with the Hubbard and t - J Hamiltonians, and a much broader range of temperatures can be explored as well. Our results

establish the spin-fermion model as a qualitatively realistic model for cuprates.

ACKNOWLEDGMENTS

We would like to acknowledge useful comments by E. Dagotto, A. Millis, and D. Scalapino. A.M. is supported by NSF under Grant No. DMR-0122523. Additional support is provided by the National High Magnetic Field Lab and MARTECH.

-
- ¹G.A. Thomas, J. Orenstein, D.H. Rapkine, M. Capizzi, A.J. Millis, R.N. Bhatt, L.F. Schneemeyer, and J.V. Waszczak, Phys. Rev. Lett. **61**, 1313 (1988); T. Timusk, S.L. Herr, K. Kamarás, C.D. Porter, D.B. Tanner, D.A. Bonn, J.D. Garrett, C.V. Stager, J.E. Greedan, and M. Reedyk, Phys. Rev. B **38**, 6683 (1988); R.T. Collins, Z. Schlesinger, F. Holtzberg, P. Chaudhari, and C. Feild, *ibid.* **39**, 6571 (1989); S.L. Cooper, G.A. Thomas, J. Orenstein, D.H. Rapkine, M. Capizzi, T. Timusk, A.J. Millis, L.F. Schneemeyer, and J.V. Waszczak, *ibid.* **40**, 11 358 (1989); Z. Schlesinger, R.T. Collins, F. Holtzberg, C. Feild, G. Koren, and A. Gupta, *ibid.* **41**, 11 237 (1990); J. Orenstein, G.A. Thomas, A.J. Millis, S.L. Cooper, D.H. Rapkine, T. Timusk, L.F. Schneemeyer, and J.V. Waszczak, *ibid.* **42**, 6342 (1990); R.T. Collins, Z. Schlesinger, F. Holtzberg, and C. Feild, *ibid.* **43**, 8701 (1991).
- ²S.L. Cooper, G.A. Thomas, J. Orenstein, D.H. Rapkine, A.J. Millis, S-W. Cheong, and A.S. Cooper, Phys. Rev. B **41**, 11 605 (1990).
- ³S. Uchida, T. Ido, H. Takagi, T. Arima, Y. Tokura, and S. Tajima, Phys. Rev. B **43**, 7942 (1991).
- ⁴I. Sega and P. Prelovsek, Phys. Rev. B **42**, 892 (1990); A. Moreo and E. Dagotto, *ibid.* **42**, 4786 (1990); W. Stephan and P. Horsch, *ibid.* **42**, 8736 (1990).
- ⁵C.-X. Chen and H.B. Schüttler, Phys. Rev. B **43**, 3771 (1991).
- ⁶J. Riera and E. Dagotto, Phys. Rev. B **50**, 452 (1994).
- ⁷E. Dagotto, Rev. Mod. Phys. **66**, 763 (1994).
- ⁸D. Scalapino, S. White, and S.C. Zhang, Phys. Rev. Lett. **68**, 2830 (1992).
- ⁹C. Buhler, S. Yunoki, and A. Moreo, Phys. Rev. B **62**, R3620 (2000).
- ¹⁰M. Moraghebi, S. Yunoki, and A. Moreo, Phys. Rev. B **63**, 214513 (2001).
- ¹¹M. Moraghebi, S. Yunoki, and A. Moreo, Phys. Rev. Lett. **88**, 187001 (2002).
- ¹²C. Buhler, S. Yunoki, and A. Moreo, Phys. Rev. Lett. **84**, 2690 (2000).
- ¹³P. Monthoux and D. Pines, Phys. Rev. B **47**, 6069 (1993); A. Chubukov, *ibid.* **52**, R3840 (1995); S. Klee and A. Muramatsu, Nucl. Phys. B **473**, 539 (1996).
- ¹⁴J.R. Schrieffer, J. Low Temp. Phys. **99**, 397 (1995); B.L. Altshuler, L.B. Ioffe, and A.J. Millis, Phys. Rev. B **52**, 5563 (1995).
- ¹⁵E. Dagotto, S. Yunoki, A.L. Malvezzi, A. Moreo, J. Hu, S. Capponi, D. Poilblanc, and N. Furukawa, Phys. Rev. B **58**, 6414 (1998).
- ¹⁶G. D. Mahan, *Many-Particle Physics* (Plenum Press, New York, 1986).
- ¹⁷We have observed similar qualitative behavior on 8×8 lattices, indicating that there are no strong finite-size effects.
- ¹⁸E. Dagotto, T. Hotta, and A. Moreo, Phys. Rep. **344**, 1 (2001).
- ¹⁹In 8×8 clusters, the behavior of the Drude weight with temperature is qualitatively similar, although the absolute value of D is smaller suggesting that it scales with lattice size.
- ²⁰E. Dagotto, A. Moreo, F. Ortolani, J. Riera and D.J. Scalapino, Phys. Rev. B **45**, 10 107 (1992).
- ²¹A.V. Puchkov, P. Fournier, T. Timusk, and N.N. Kolesnikov, Phys. Rev. Lett. **77**, 1853 (1996).
- ²²T. Startseva, T. Timusk, A.V. Puchkov, D.N. Basov, H.A. Mook, M. Okuya, T. Kimura, and K. Kishio, Phys. Rev. B **59**, 7184 (1999); T. Startseva, T. Timusk, A.V. Puchkov, D.N. Basov, H.A. Mook, T. Kimura, and K. Kishio, cond-mat/9706145 (unpublished).
- ²³A.V. Puchkov, D.N. Basov, and T. Timusk, J. Phys.: Condens. Matter **8**, 10 049 (1996).
- ²⁴S. Herr, K. Kamarás, C. Porter, M. Doss, D. Tanner, D. Bonn, J. Greedan, C. Stager, and T. Timusk, Phys. Rev. B **36**, 733 (1987); J. Orenstein, G. Thomas, D. Rapkine, C. Bethea, B. Levine, R. Cava, E. Reitman, and D. Johnson, Jr., *ibid.* **36**, 733 (1987).
- ²⁵B. Battlog, H. Takagi, H.Y. Hwang, R.J. Cava, H.L. Kao, and J. Kwo, Physica C **235-240**, 130 (1994); H. Takagi, B. Batlogg, H.L. Kao, J. Kwo, R.J. Cava, J.J. Krajewski, and W.F. Peck, Jr., Phys. Rev. Lett. **69**, 2975 (1992).